

Supplementary Information

Small-angle X-ray scattering (SAXS) measurements were performed on a D8 DISCOVER-Bruker instrument at 40 kV and 40 mA. Powder patterns were recorded in capillary transmission configuration by using a Göbel mirror (Cu K α 1 radiation) and the LYNXeye detector. The powder patterns were recorded between 0.2 and 10 ° in 2 θ with a total measuring time of 120 min.

Powder X-ray diffraction was used to study the crystallinity of Nb-based catalysts supported on porous silicas, with a PANalytical X'Pert PRO diffractometer, with a germanium monochromator and Cu K α (1.5406 Å) radiation.

The catalyst morphology was evaluated by TEM-EDS, with a FEI Talos F200X, which combines a high-resolution STEM, TEM imaging, and an energy dispersive X-ray spectroscopy (EDS) signal detection. The 3D chemical characterization was obtained from the compositional mapping. The samples were dispersed in ethanol and a drop of the suspension was put on a Formvar/carbon supported Cu grid (300 mesh).

Textural parameters were analyzed by adsorption-desorption of N₂ at -196 °C, using an automatic ASAP 2020 Micromeritics. Samples were previously outgassed overnight at 150 °C and 10⁻⁴ mbar. The de Boer's t-plot method was used to obtain the micropore surface areas, whereas the specific surface area was deduced from the Brunauer-Emmett-Teller equation (BET), considering a N₂ cross section of 16.2 Å². The Nonlocal Density Functional Theory (NLDFT) was applied to determine the pore size distribution from the desorption branch of the isotherm. The total pore volume was deduced from N₂ adsorbed at P/P₀ = 0.996.

A Physical Electronics PHI5700 spectrometer, with non-monochromatic Mg K α radiation (300 W, 15 kV, and 1253.6 eV) and a multichannel detector, was employed to obtain the X-ray photoelectron spectra. A constant pass energy mode at 29.35 eV, with a 720 μ m diameter analysis area, was used for recording the spectra. Acquisition and data analysis were performed with a PHI ACCESS ESCA-V6.0F software package, whereas charge referencing was measured against adventitious carbon (C 1s at 284.8 eV). A Shirley-type background was subtracted from the signals, and the fitting of recorded spectra was carried out with Gaussian-Lorentzian curves, for a better determination of different binding energies.

The total amount of acid sites was determined by thermo-programmed desorption (NH₃-TPD) in a AutoChem II 2920 equipment. For each study, about 50 mg of sample was cleaned with He flow (50 mL/min) with a rate of 30 °C/min until 550 °C, maintaining this temperature for 15 min. Then, the sample was cooled down to 80 °C in He under the same flow. In the next step, the sample was undergone to a NH₃/He (10% vol. NH₃) flow (50 mL/min) at 80 °C for 20 min. After that, a flow of He of was passed 50 mL/min to 90 min, to eliminate the physisorbed NH₃. Finally, the sample was heated from 80 to 550 °C, monitoring the NH₃-desorbed by thermal conductivity detector (TCD).

FTIR spectra of adsorbed pyridine were recorded on aVertex70 FT-IR spectrophotometer model supplied by Bruker. Self-supported wafers of the samples with a weight/surface ratio of approximately 15 mg/cm² were placed in a vacuum cell with greaseless stopcocks and CaF₂ windows. The samples were evacuated at 250 °C and 10⁻² Pa overnight, before they were exposed to pyridine vapors at room temperature for 15 min and then outgassed at 200 °C.

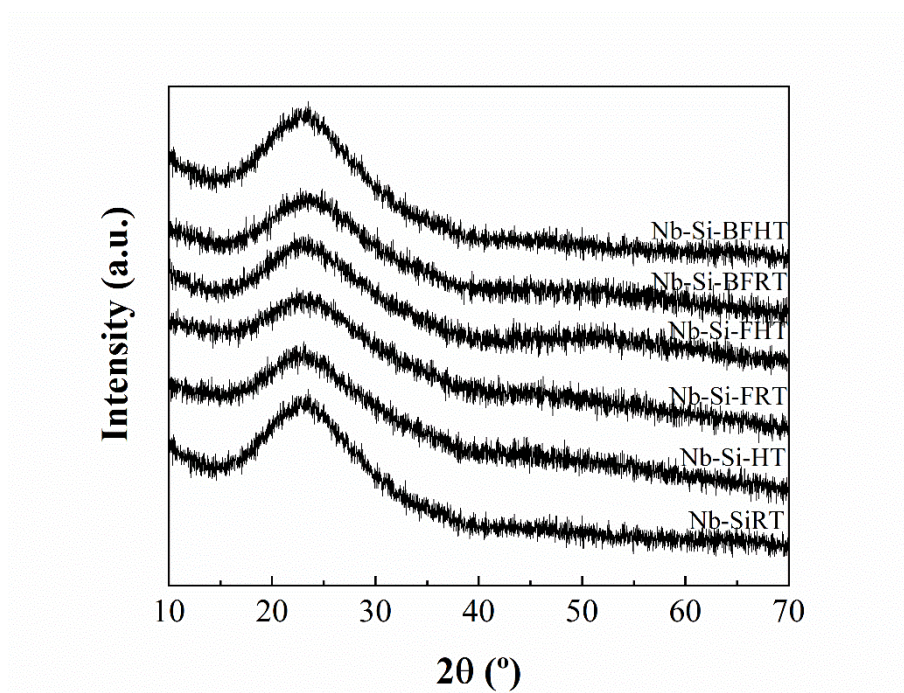


Figure S1. X-ray diffractograms of Nb-based catalysts supported on porous silicas.

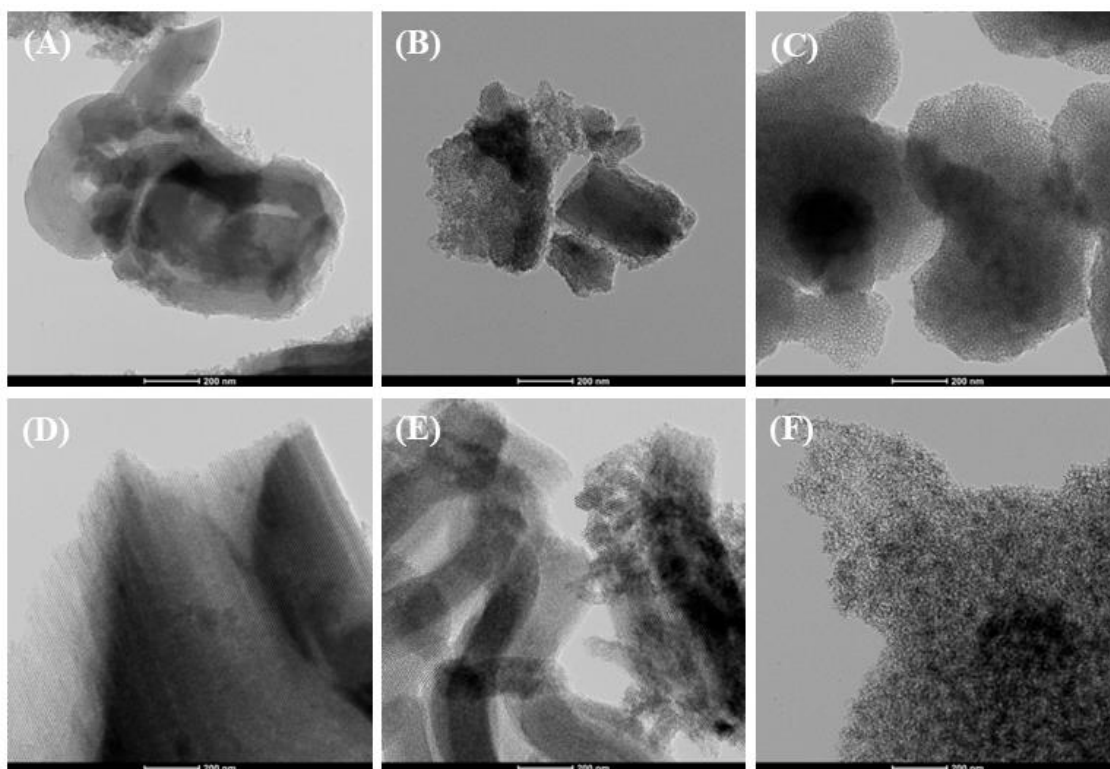


Figure S2. TEM micrographs of the Nb-based catalysts supported on porous silicas (Scale: 200 nm). A) Nb-Si-RT, B) Nb-Si-FRT, C) Nb-Si-BFRT, D) Nb-Si-HT, E) Nb-Si-FHT and F) Nb-Si-BFHT.

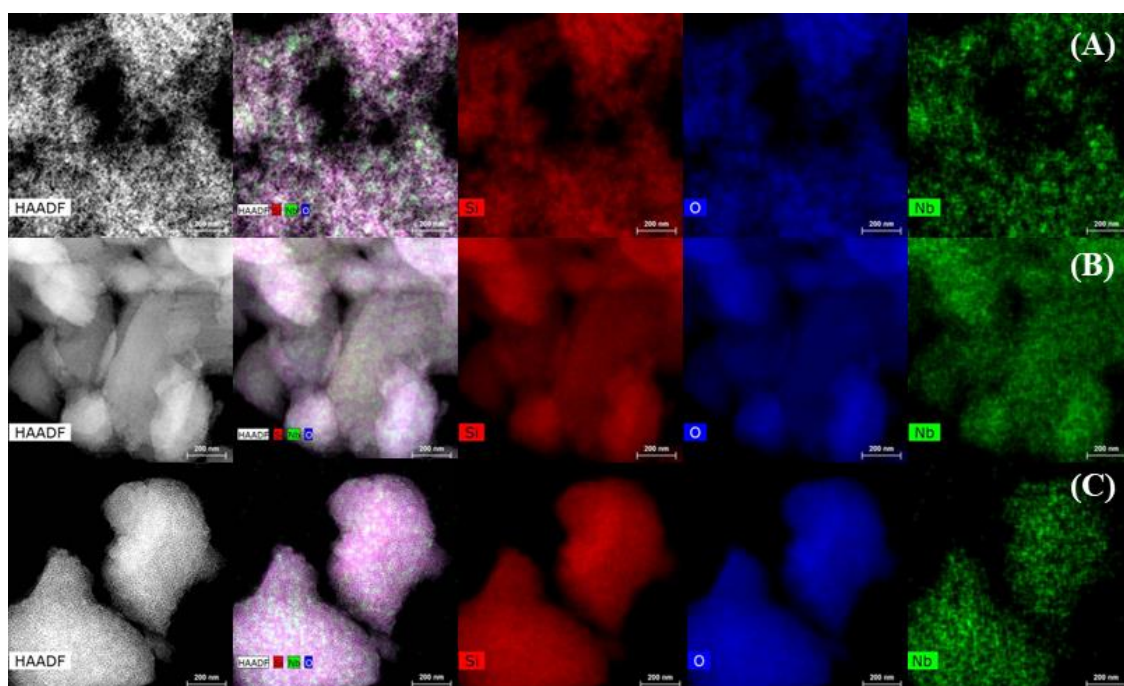


Figure S3. Mapping obtained from S-TEM micrographs of A) Nb-Si-RT, B) Nb-Si-FRT, and C) Nb-Si-BFRT catalysts. (Scale: 200 nm).

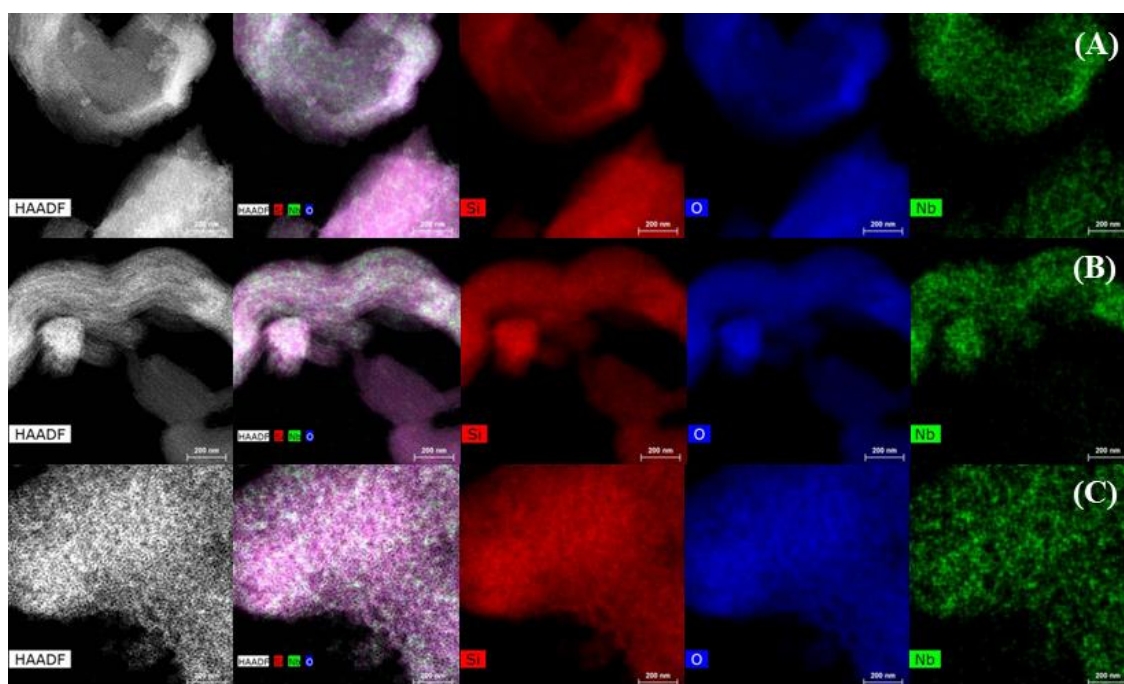


Figure S4. Mapping obtained from S-TEM micrographs of A) Nb-Si-HT, B) Nb-Si-FHT, and C) Nb-Si-BFHT catalysts. (Scale: 200 nm).

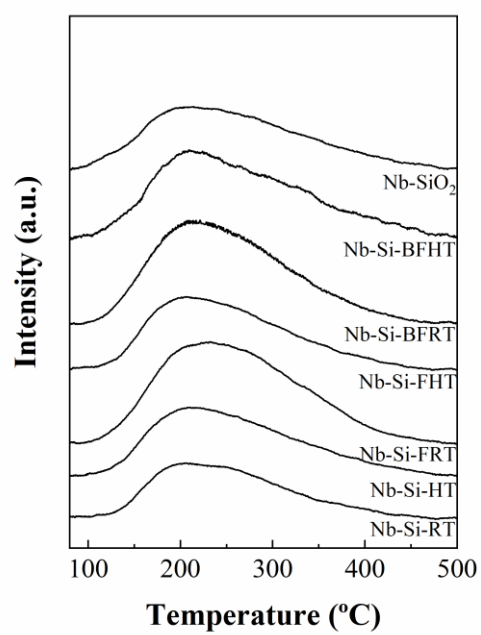


Figure S5. NH₃-Thermoprogammed desorption of Nb-based catalysts supported on porous silicas.

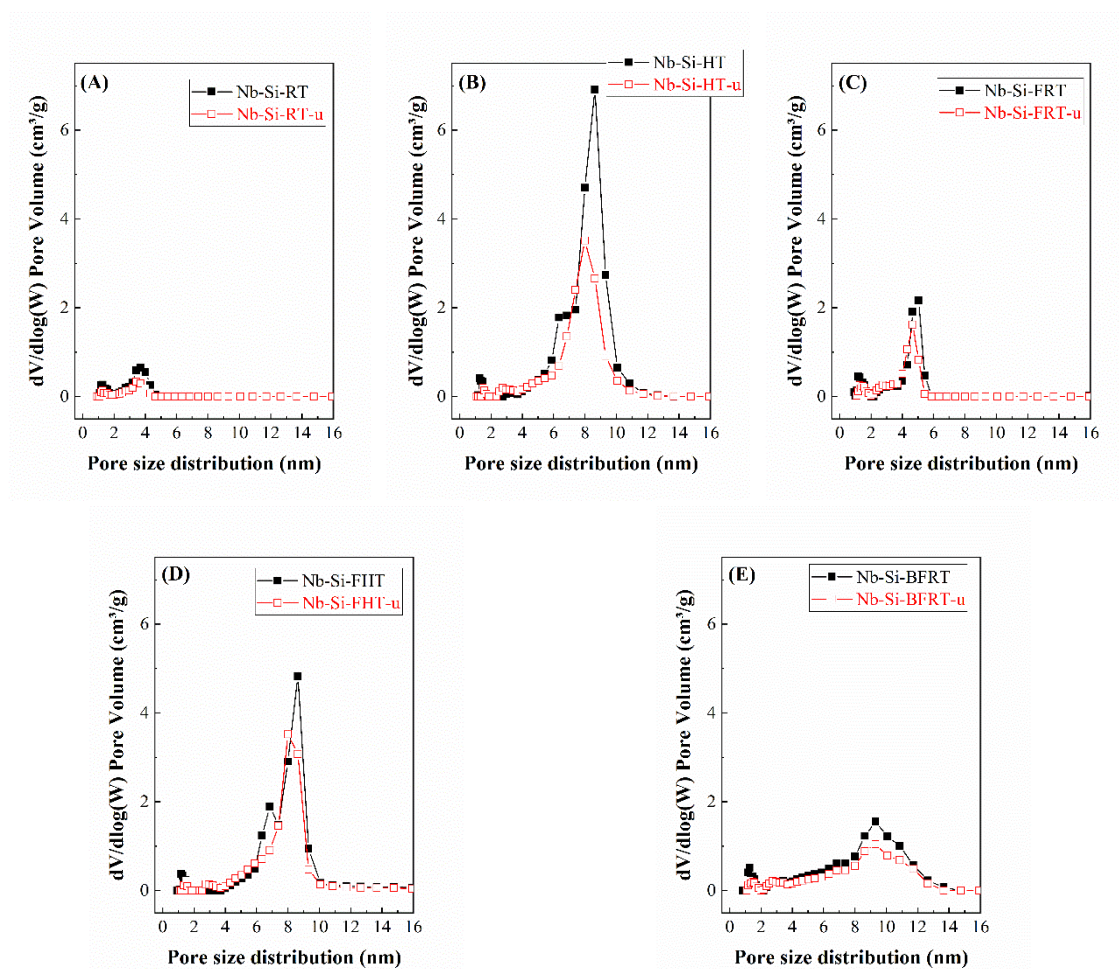


Figure S6. Comparison of the pore size distribution estimated by the DFT method for the Nb-based catalysts supported on porous silica before and after the reaction at 170 °C for (A) Nb-Si-RT, (B) Nb-Si-HT, (C) Nb-Si-FRT, (D) Nb-Si-FHT and (E) Nb-Si-BFRT catalysts.